Current Science
CS 5 (6), 5538-5550 (2025)
Received 24 November 2025 | **Accepted 18 December** 2025 | **Online Available 21 December** 2025
https://doi.org/10.52845/CS/2025-5-6-20

Current Science
Current Science

OPEN ACCESS
ISSN (O) 2795-8639

Original Article

Novel Compound Heterozygous EVC1 Mutations Cause Ellis-Van Creveld Syndrome in a Chinese Prenatal Fetus

Haiyan Luo[1], Zhen Guo[1], Yao Yu[2], Jia Chen[1], Qing Lu[1], Yan Yang[1], Ting Huang[1], Danping Liu[1], Wangli Nie[3], Bicheng Yang, Jun Zou, Yanqiu Liu[1#], Yongyi Zou[1#]

[1]Jiangxi Maternal and Child Health Hospital, Nanchang, 330006, Jiangxi Province, China

[2]Jiujiang Polytechnic University of Science and Technology, Gongqing, 332020, Jiangxi Province, China

[3]Jiujiang Maternal and Child Health Hospital, 332000, Jiangxi Province, China

***Corresponding Author: Prof. Yanqiu Liu, Dr Yongyi Zou**

Abstract:
Fetal genetic skeletal disorders are common congenital anomalies with notable genetic and phenotypic heterogeneity. Genetic analysis plays an important role in the definitive diagnosis of these skeletal conditions. In the present study, fetal development was assessed by routine ultrasonography at 16+5 weeks of gestation. Amniocentesis was performed, followed by comprehensive genetic assessment including chromosomal karyotyping, chromosomal microarray analysis (CMA) and whole-exome sequencing (WES). Variants initially identified by WES were subsequently validated using Sanger sequencing or RT-qPCR. *In vitro* investigations on the newly identified variant were further conducted by RT-qPCR and western blotting (WB) analysis. Preimplantation genetic testing (PGT) for the diagnosed monogenic disease was conducted based on next-generation sequencing (NGS)-based single nucleotide polymorphism haplotype analysis and Sanger sequencing. Meanwhile, PGT for aneuploidy screening was performed by NGS. Prenatal diagnosis was further conducted for validation of the PGT results using a combination of Sanger sequencing, RT-qPCR, CMA and chromosomal karyotyping. Routine second-trimester prenatal ultrasound examination identified shortened limbs (<-2.0 standard deviations) in the fetus. Chromosomal karyotyping and CMA identified no genetic aberrations, whilst WES revealed compound heterozygous variants in *EVC1* in the affected fetus. These included a novel frameshift variant (c.130delC, p.Leu44Phefs*72) and a previously reported heterozygous multiexon deletion spanning exons 9-11, both of which were validated by Sanger sequencing and RT-qPCR, respectively. *In vitro* RT-qPCR demonstrated that the variant c.130delC had no impact on the transcriptional expression of the *EVC1* gene, whilst WB demonstrated the accumulation of truncated protein isoforms. Combined genetic and pedigree analysis indicated a diagnosis of Ellis-van Creveld (EvC) syndrome in the fetus. After thorough genetic counseling, the affected pregnancy was terminated. PGT established a subsequent singleton pregnancy not affected by EvC syndrome or chromosomal aneuploidies, which was confirmed by further prenatal diagnosis. The present study identified and characterized a novel mutation in the *EVC1* gene, which has broadened the established mutational spectrum of EvC syndrome, and holds notable implications for the clinical management and genetic counseling of families affected by EvC syndrome.

Keywords: Ellis-van Creveld Syndrome, prenatal diagnosis, WES, novel mutation; preimplantation genetic testing

1. Introduction

Genetic skeletal dysplasia represents a heterogeneous group of genetic disorders. The

overall incidence of these conditions is estimated at ~1/5,000 births, accounting for nearly 10% of prenatal mortality [1]. Ellis-van Creveld (EvC) syndrome (OMIM 225500) is an autosomal recessive congenital skeletal disorder with an estimated incidence of ~1/60,000 live births in the general population. Notably, the prevalence is markedly higher in the Old Order Amish population of Lancaster County (Pennsylvania, USA), reaching ~5/1,000 live births [2,3]. EvC syndrome demonstrates substantial genetic heterogeneity, with ~70% of the cases resulting from nonsense or frameshift mutations and leading to loss-of-function alterations in either the EVC1 or EVC2 gene.

EvC syndrome may be diagnosed prenatally based on characteristic ultrasound findings including a hypoplastic thorax resulting from short ribs, shortened limbs, frequent polydactyly and associated visceral anomalies. Fetal structural abnormalities of EvC syndrome, particularly limb shortening can be detected as early as week 15 of gestation. However, additional anomalies such as a narrow thorax, hexadactyly of the hands or feet and cardiac defects are typically detectable during anomaly scans performed during weeks 22-28 of gestation in China [4,5]. The lack of a family history, together with the nonspecific and subtle sonographic features of EvC syndrome on routine second-trimester ultrasound, poses notable challenges for conclusive diagnosis during the early stages. This often leads to considerable psychological distress for expectant parents and increases the maternal risks when late-term pregnancy termination is carried out. Therefore, the integration of genetic testing with the sonographic detection of shortened limbs is crucial for the early and conclusive diagnosis of EvC syndrome in the second trimester. Recent breakthroughs in next-generation sequencing (NGS) technologies have brought high-throughput genomic interrogation approaches, especially whole exome sequencing (WES), to the forefront of clinical diagnostics. These technologies provide high efficiency and cost-effectiveness in identifying pathogenic variants and improving the molecular characterization of various genetic disorders [6-8]. Growing evidence from large-scale cohort studies indicates that WES attains a diagnostic yield ranging 65.8-83.3% in the prenatal diagnosis of fetal skeletal system abnormalities. These findings underscore the clinical value of WES in perinatal genetic diagnosis [9-11].

To date, a total of 72 distinct pathogenic variants in the EVC1 gene have been documented as being linked to EvC syndrome in the professional Human Gene Mutation Database (http://www.hgmd.cf.ac.uk/ac/all.php). Despite the advancements made in molecular profiling, only nine disease-associated mutations in EVC1 have been well-characterized within Chinese populations. This limited genetic understanding highlights the critical need for expanded research to fully elucidate the mutational spectrum of EVC1 within this demographic. Such efforts are crucial for establishing robust frameworks to support precision genetic counseling and evidence-based clinical management [12-17]. In the present study, a novel frameshift mutation EVC1 c.130delC identified in a Chinese fetus is presented, which has further broadened the mutational spectrum of EvC syndrome.

Materials and Methods

Subject and clinical information. The participant was a 28-year-old G3P0 woman at week 16 of gestation with a spontaneously conceived pregnancy. The patient denied consanguinity and reported a history of two previous pregnancies that were terminated due to fetal abnormalities. These included shortened ribs, limb hypoplasia and ventricular septal defects diagnosed at the gestational ages of 24+4 and 26+2 weeks, respectively. Nevertheless, no confirmatory prenatal genetic testing was conducted, and no archived fetal tissue samples were available for

subsequent retrospective analysis. The patient was in her third pregnancy and reported no complications during the routine prenatal visits. However, the routine second-trimester ultrasound conducted at 16+5 weeks of gestation for fetal developmental assessment showed sonographic findings indicative of fetal limb shortening. A subsequent routine ultrasound at 18+3 weeks demonstrated consistent findings. A total of two consecutive routine prenatal ultrasound scans identified fetal skeletal abnormalities, specifically shortened humerus and femur lengths, each measuring 2.0 standard deviations below the mean for gestational age. Comprehensive clinical parameters associated with these findings are presented in Table I. Prenatal ultrasonography demonstrated features indicative of fetal skeletal disorder (Fig. 1A), and a schematic pedigree of the family was presented in Fig. 1B. The collection of all biological specimens and clinical data was conducted following the acquisition of written informed consent from all participants. The present study was approved by the Ethics Committee of Jiangxi Maternal and Child Health Hospital (Nanchang, China) (No. 20210324).

Table I: Assessment of fetal clinical parameters by two consecutive ultrasonographic examinations

No	BPD (mm)	GA (W)	HC (mm)	AC (mm)	FL(mm)	HL(mm)	Clinical evaluation
1	31	16W+5	114	109	107	126	-2.0 SD
2	39	18W+3	141	118	160	140	-2.0 SD

Abbreviations: GA, gestational age; BPD, biparietal diameter; HD, head circumference; AD, abdomen circumference; HL, humerus length; FL, femur length, SD: standard deviation.

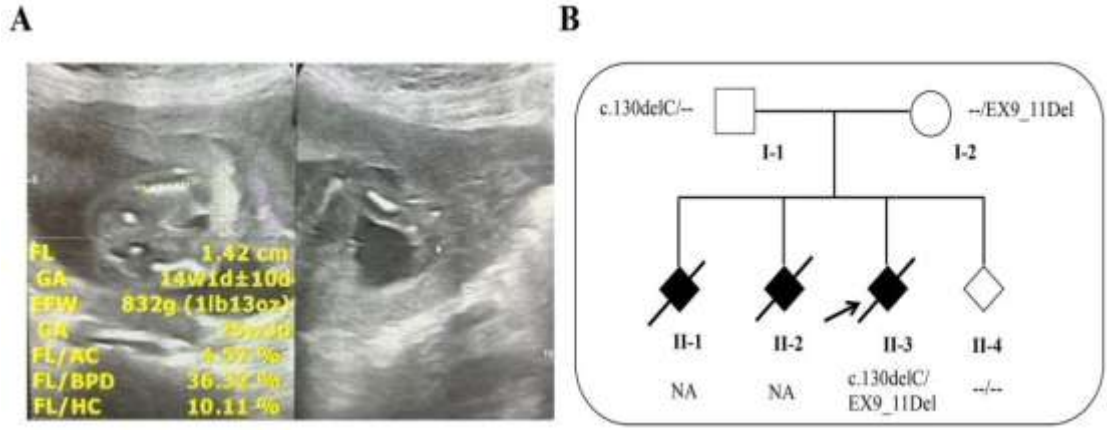

Fig 1A. Sonographic examination at 16 weeks' gestation revealed markedly shortened long bones, with both humeral and femoral lengths measuring more than 2.0 standard deviations below the gestational age-adjusted mean (<-2.0 SD). Figure 1B. In the pedigree chart, an unfilled diamond denotes a fetus of undetermined sex, while a filled diamond indicates a pregnancy that was electively terminated. Family members are designated as follows: I-1 (father of the proband), I-2 (mother of the proband); II-1 and II-2 (spontaneous abortions); II-3 (the proband); and II-4 (the embryo conceived through PGT). The notation "NA" indicates that clinical data are unavailable.

Prenatal fetal ultrasound screening. All fetal ultrasound examinations were conducted in strict adherence to standardized imaging protocols established by the Fetal Medicine Foundation. In China, routine prenatal ultrasound screening primarily involves the standard biometric measurement of key fetal growth parameters, such as biparietal diameter and femur length,

along with a comprehensive evaluation of placental location and amniotic fluid volume. However, a detailed fetal structural survey, commonly referred to as the fetal anomaly scan, is typically performed to systematically evaluate fetal anatomical structures for malformations. This comprehensive examination is generally conducted during two designated gestational periods: 20-24+6 weeks and 26-30 weeks.

WES and the integrated bio-informatics pipeline. WES was conducted by Illumina, Inc., with an average depth of 200x, covering 95% of the target regions. Genomic DNA was fragmented using a S220 focused-ultrasonicator (Covaris, LLC) and subsequently enriched using the SureSelect Human All Exon V6 Kit (Agilent Technologies, Inc.). Paired-end libraries were sequenced on an Illumina HiSeq 2500 platform (Illumina, Inc.), generating 101-bp paired-end reads. Quality-controlled sequencing reads were aligned to the human reference genome (hg19/GRCh37) using NOVOAlign. Variant calling was performed using the Genome Analysis Toolkit. Variants identified were subsequently filtered to exclude those with a minor allele frequency >0.001 in either the Genome Aggregation Database or the Chinese Exome Sequence Database. Synonymous variants without predicted splicing effects were also removed. Deleterious single-nucleotide variants were prioritized using multiple prediction algorithms, including SIFT, PolyPhen-2, MutationTaster and PROVEAN. Potential inherited mutations and de novo mutations associated with skeletal dysplasia were then screened using the MIRTrios program.

Validation of causative mutations identified by WES. The causative variants primarily identified by WES were further validated by Sanger sequencing or RT-qPCR. Sanger sequencing was performed on an Applied Biosystems 3500 DX Genetic Analyzer (Thermo Fisher Scientific, Inc.) and the resulting chromatograms were aligned and compared against the reference transcript sequence. Exon-level deletions or duplications by RT-qPCR were quantified in a Bio-Rad iCycler real-time PCR detection system (Bio-Rad Laboratories, Inc.) using SYBR Green I dye, with a specific primer pair for each exon. To normalize for potential variations in DNA input or the presence of PCR inhibitors, the reference gene HBB was amplified and quantified in parallel reactions for each sample. The sequences of the primers used for PCR are provided in Table II.

Table II Primers used in the study

Primers	Primer Length (bp)	Sequence(5’-3’)
EVC-EX1-F	20	AAGGGGAGAGAAGCAGGAGT
EVC-EX1-R	20	TGTCAAGGATCACCCAACGG
EVC-EX9-F	20	CAGCTATGGTCCTGTGTGTT
EVC-EX9-R	20	CTGGACTTGCAGCTTCAGAA
EVC-EX10-F	19	ATCCCAGAGTTTGTCCAGCG
EVC-EX10-R	20	CTCTGTTCCTCCTCTTGGGC
EVC-EX11-F	20	AGGAGAATGTCAGAGCCACC
EVC-EX11-R	20	GTTCTCGCACACACACAGAC
HBB-EX2-F	21	TGACTCTCTCTGCCTATTGGTCTA
HBB-EX2-R	24	TTAGGGTTGCCCATAACAGCA

Construction of expression vectors and cell transfection. The recombinant vector pEGFP-C1 EVC1 wt was constructed by inserting the full-length human EVC1 complementary DNA (cDNA) into the pEGFP-C1 plasmid using HindIII and KpnI restriction sites for subsequent expression. The c.130delC (p.Leu44Phefs*72)

mutation was subsequently introduced into this vector by site-directed mutagenesis (Baiyi Biopharm Co., Ltd.) to generate the mutant construct pEGFP-C1 EVC1 mut. Both the wild-type and mutant eukaryotic expression vectors were transiently transfected into HEK293T cells using Lipofectamine 2000.

In vitro RNA analysis and western blotting (WB). Total RNA was extracted from cell samples 48 h after transfection using the Trizol reagent (Invitrogen; Thermo Fisher Scientific, Inc.). cDNA was synthesized in accordance with the manufacturer's protocol (Takara Biotechnology Co., Ltd.). The mRNA expression levels of wild-type and mutant target genes were then analyzed by RT-qPCR on an ABI StepOne Real-Time PCR system (Applied Biosystems) using SYBR Green Realtime PCR Master Mix (LMAI Bio). Subsequently, at 36 h post-transfection with either wild-type or mutant recombinant expression vectors, total protein was isolated from cell pellets using RIPA lysis buffer. Differential protein expression between wild-type and mutant constructs was assessed by western blot analysis following standard procedures.

Preimplantation genetic testing (PGT). NGS-based single nucleotide polymorphism (SNP) haplotyping was performed on the prospective parents and an affected family member to delineate the chromosomal haplotypes associated with the normal and disease-associated haplotypes. The target gene, along with >200 informative SNPs within 2 Mb range were sequenced by NGS (Peking Jabrehoo Med-Tech Co., Ltd) to identify disease-associated and normal haplotypes within the family. Only heterozygous SNPs were considered informative for haplotype phasing. Subsequently, blastocysts that survived until day 5 underwent laser-assisted hatching and trophectoderm biopsy. The biopsied samples were subjected to whole-genome amplification via multiple displacement amplification and whole genome amplification. After which, the amplified products were used for comprehensive genomic analyses, including SNP haplotyping, Sanger sequencing, aneuploidy screening and copy number variation analysis. Embryos with the normal SNP haplotypes identified by NGS were selected and further confirmed by Sanger sequencing. Additionally, low-coverage whole-genome NGS was employed to detect chromosomal aneuploidies and structural imbalances >1 Mb for PGT for aneuploidy. Ultimately, only embryos negative for two causative variants in EVC1 and free of chromosomal aneuploidies were considered suitable for transfer.

Confirmation of PGT results by prenatal diagnosis. Amniocentesis was performed at week 18 of gestation to further validate the genetic results of the PGT conducted on the transferred blastocyst. The two causative mutations in EVC1 were detected using Sanger sequencing and RT-qPCR. Concurrently, conventional G-banded karyotyping with a resolution of 10 Mb was carried out for the detection of chromosomal aberrations. Moreover, chromosomal microarray analysis (CMA) was performed with CytoScan 750K arrays (Affymetrix; Thermo Fisher Scientific, Inc.) to detect clinically significant genomic copy number variants.

Statistical analysis. Statistical analysis was performed using GraphPad Prism 8 software (Dotmatics). Measurement data were presented as the mean ± standard deviation. Differences among groups were compared using one-way analysis of variance, followed by the Least Significant Difference post hoc test for pairwise comparisons. $P<0.05$ was considered to indicate a statistically significant difference.

Results

Variant interpretation and annotation. WES identified two compound heterozygous variants, c.130delC (p.Leu44Phefs*72, inherited paternally) and EX9_EX11 Del (inherited

maternally), in EVC1 as the primary findings. Additionally, the secondary findings reported four heterozygous variants: c.413G>A (p.Arg138His, inherited paternally) in COL9A3, c.1141G>A (p.Ala381Thr, inherited maternally) in FLNA, c.1232A>T (p.His411Leu, inherited paternally) in MMP9 and c.1687G>A (p.Glu563Lys, inherited maternally) in ROR2. The unreported variant c.130delC and the previously documented exons 9-11 deletion in EVC1 were both classified as pathogenic (PVS1 + PM2 + PM3), while the other four heterozygous variants were reported as variants of uncertain significance according to American College of Medical Genetics and Genomics (ACMG)/AMP guidelines (2015) [18]. Furthermore, the novel c.130delC variant was not detected in 200 ethnically matched, unaffected controls. Routine prenatal ultrasound examination during the second trimester revealed notable shortening of the fetal limbs, showing partial overlap with features of EvC syndrome, as other characteristic phenotypic manifestations may not yet be detectable by routine ultrasound. Therefore, by combining the fetal phenotypes and co-segregation analysis in the family, it was hypothesized that the two compound variants in EVC1 are likely causative genetic factors underlying the observed fetal skeletal anomalies in the affected fetus.

Validation of two heterozygous variants by Sanger sequencing and RT-qPCR. Point mutation and multi-exon deletion analyses were confirmed using Sanger sequencing and RT-qPCR, respectively. Sanger sequencing confirmed the presence of c.130delC (p.Leu44Phefs*72) in the proband and the father, whereas the mother carried the wild-type allele at this locus (mutation sites were indicated by arrows; Fig. 2A and B). RT-qPCR analysis of genomic DNA revealed an ~50% reduction in the copy number of exons 9-11 in both the proband and the mother compared with the father, which was consistent with the findings from WES.

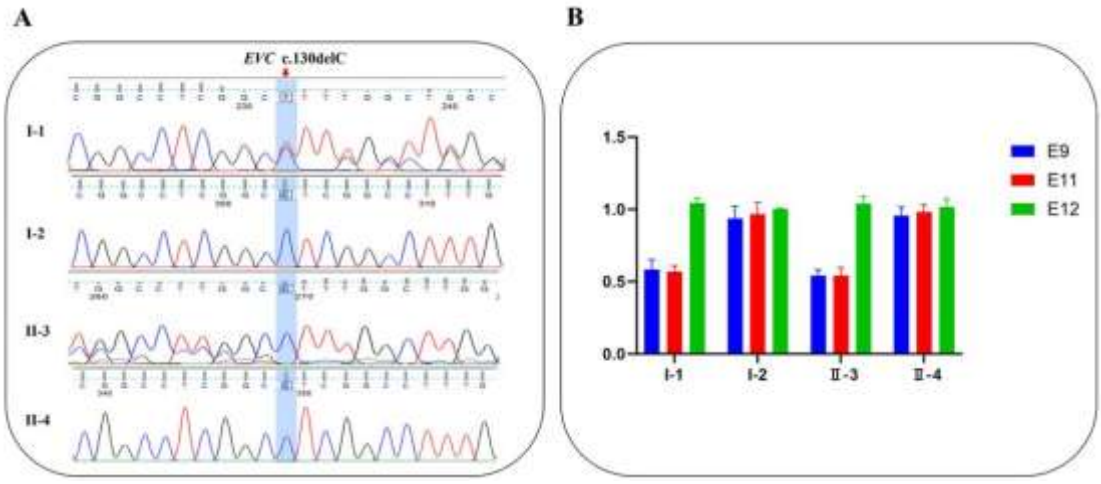

Fig 2. Figure 2A presents DNA sequence analysis of the *EVC1* c.130delC variant. The upper panel depicts the wild-type nucleotide sequence (control), while the lower panel corresponds to a heterozygous carrier. Figure 2B shows copy number analysis of *EVC1* exons 9-11 by RT-qPCR performed on genomic DNA from the proband and parents.

In vitro RNA analysis and WB. The constructed eukaryotic expression vectors for wild-type (pEGFP-C1 *EVC1* wt) and mutant (pEGFP-C1 *EVC1* c.130delC, p.Leu44Phefs*72) were validated by Sanger sequencing (Fig. 3A). RT-qPCR analysis revealed no significant difference in mRNA expression levels between the wild-type and mutant (c.130delC) *EVC1* genes in HEK293T

cells (Fig. 3B), suggesting that this mutation may not affect *EVC1* transcription. WB confirmed that the mutation c.130delC introduced a premature termination codon and resulted in the production of a truncated protein (GFP-*EVC1*-mut1, ~15 kDa), in contrast to the full-length wild-type protein (GFP-*EVC1*-wt, ~112 kDa). Notably, the expression level of the truncated mutant protein was markedly increased compared with that of the wild-type protein (Fig. 3C).

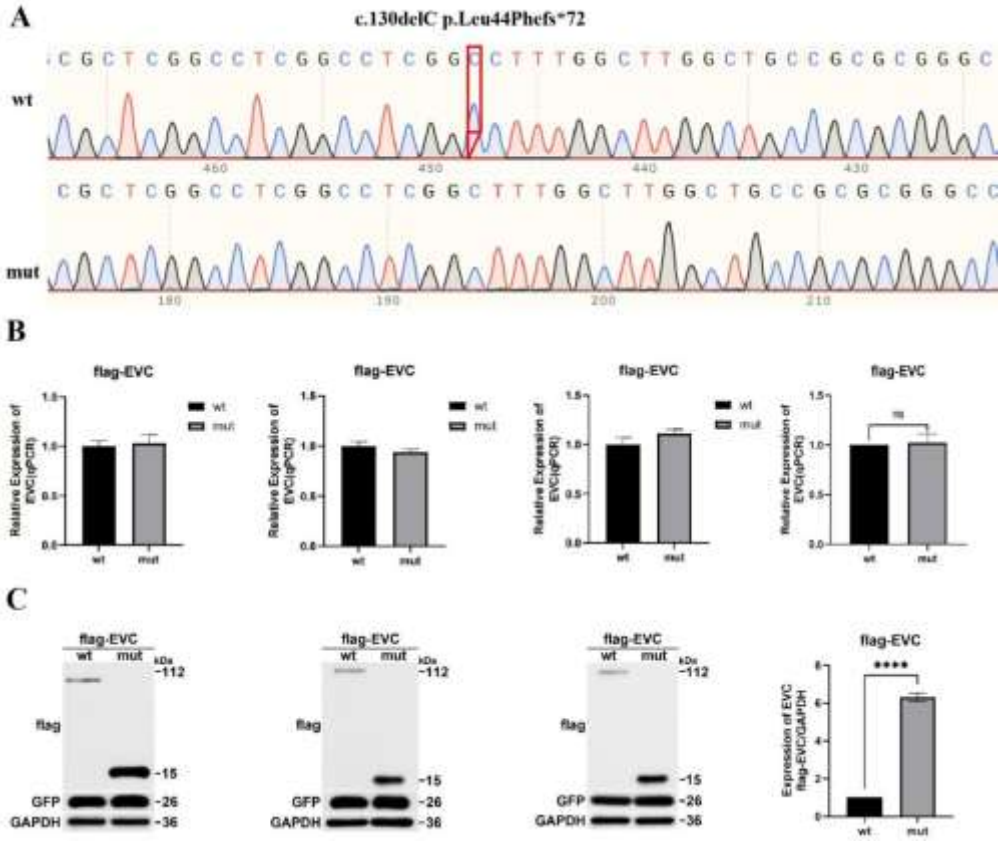

Fig. 3 Figure 3A: Sequencing analysis confirmed the successful introduction of the c.130delC (p.Leu44Phefs*72) mutation. Figure 3B: RT-qPCR revealed no significant difference in *EVC1* mRNA expression between the mutant and wild-type cells. Figures 3C: Western blot analysis performed in three independent replicates revealed significant accumulation of truncated Evc protein in the *EVC1*-mutant (mut) HEK293T cells.

PGT and prenatal diagnosis. In the PGT cycle, three embryos developed to the blastocyst stage and underwent trophectoderm biopsy. Genetic analysis yielded conclusive results for all three embryos. Haplotype linkage analysis revealed that Embryo 1 carried the maternal at-risk SNP haplotype, indicating the presence of the heterozygous EX9_EX11 deletion in the *EVC1* gene associated with EvC syndrome. Embryos 2 and 3 carried maternal and paternal wild-type haplotypes and were therefore genetically unaffected by EvC syndrome (Fig. 4). Concurrent PGT for aneuploidy analysis demonstrated that Embryo 1 was monosomic for chromosome 22 (45,XN,-22), whereas Embryos 2 and 3 exhibited a euploid karyotype. Following comprehensive genetic screening, Embryo 3 was prioritized for transfer based on its euploid status and the absence of causative *EVC1* mutations. Subsequent prenatal diagnosis via amniocentesis at 18+3 weeks of gestation confirmed a normal fetal genotype without genomic aberrations. Both G-banding karyotyping and CMA analysis of fetal amniotic cells revealed no abnormalities. A

healthy male infant was born and has remained well with normal findings on all routine physical examinations to date.

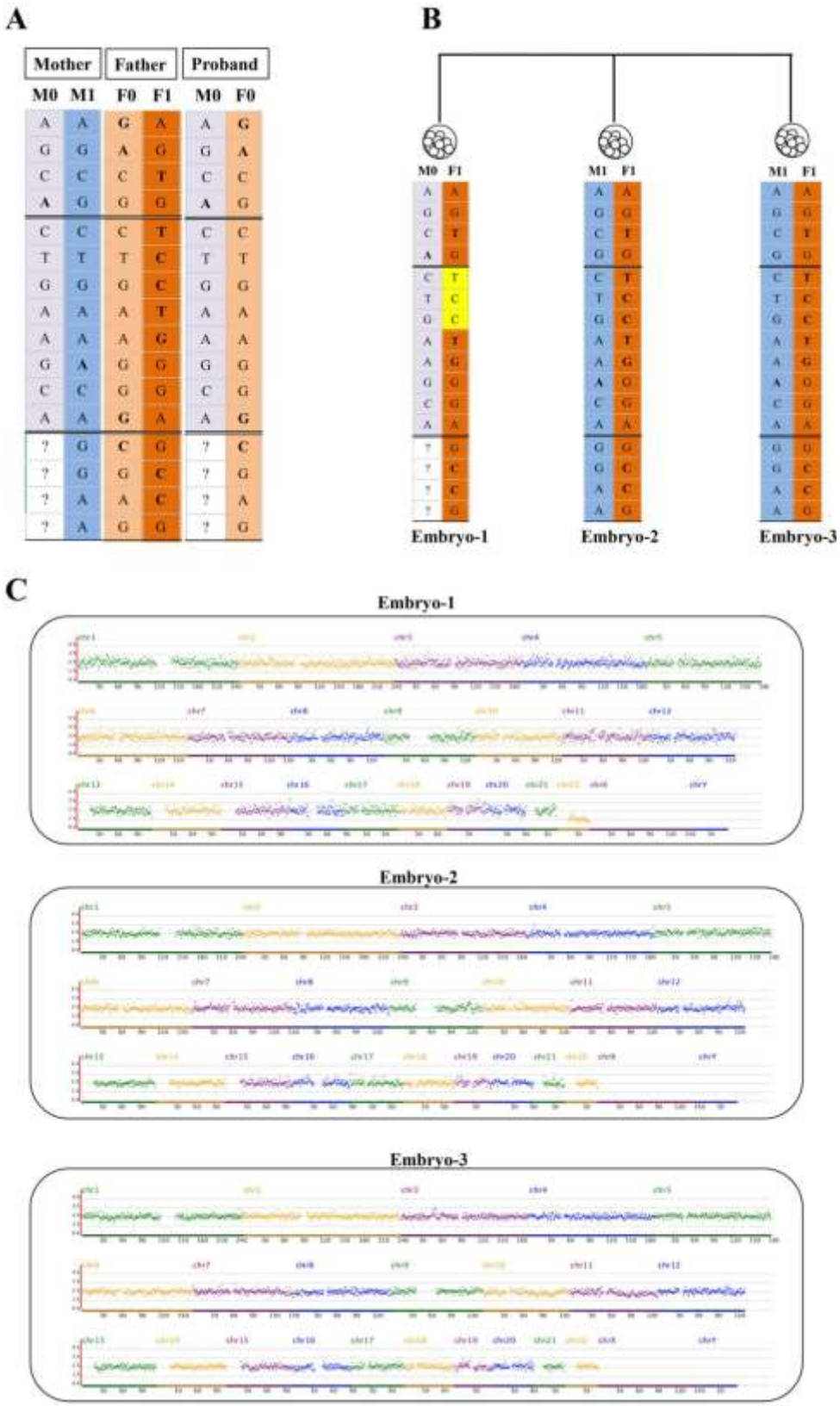

Fig 4. 4A: Haplotype-based linkage analysis performed for the *EVC1* gene using DNA from the proband and the unaffected parents. M0 and F0 denote the maternal and paternal at-risk alleles on chromosome 4, respectively, whereas M1 and F1 denote the corresponding non-risk alleles. Figure

4B: The SNP-haplotype linkage analysis for the three embryos. Figure 4C: Screening results of the PGT-A, with the X-axis representing the chromosome number (1-22) and the Y-axis indicating chromosomal gain (+) or loss (-). Information regarding sex chromosomes is omitted in compliance with regulations governing maternal and infant health care in mainland China.

Discussion

The EVC1 gene (OMIM *604831), located on chromosome 4q16, spans ~120 kb of genomic DNA and comprises 21 coding exons. It encodes a 992-amino acid protein featuring a leucine zipper motif, three putative nuclear localization signal sequences and a putative transmembrane domain [19]. As a single-pass type I transmembrane protein, it demonstrates low expression levels in the heart, kidney, developing bones and lungs [20]. During bone development, EvC syndrome expression is observed in vertebral bodies, ribs and limbs, with elevated expression in distal compared with proximal regions. Localized at the base of chondrocyte cilia, the Evc protein acts as a positive mediator of the sonic hedgehog signaling pathway, which is crucial for normal endochondral ossification and skeletal morphogenesis. In vitro studies demonstrate that the Evc protein directly interacts with Evc2 to form a complex at the primary cilia membrane, which is essential for both endochondral growth and intramembranous ossification [21,22]. During murine embryonic development, Evc protein expression is observed in the secondary heart field, encompassing the outflow tract and dorsal mesenchymal protrusion, as well as in mesenchymal components of the atrial septum and atrioventricular cushions [23]. Evc-null mice recapitulate several key features resembling EvC syndrome, such as short limbs, short ribs and dental abnormalities. However, unlike the human condition, they do not exhibit polydactyly or cardiac malformations [24]. These functional studies suggest that mutations in the EVC1 gene may contribute to the pathogenesis of skeletal and cardiac hypoplasia.

Since the initial identification of the EVC1 gene in the year 2000, homozygous or compound heterozygous mutations in EVC1 have been established as the genetic cause of EvC syndrome [25]. Notably, heterozygous mutations in EVC1 are associated with Weyers acrofacial dysostosis (OMIM 193530), an autosomal dominant disorder allelic to EvC syndrome and characterized by a distinct phenotypic profile that notably excludes the narrow thorax and congenital heart defects typically observed in EvC syndrome. To date, a variety of EVC1 mutations, predominantly nonsense or frameshift variants, have been identified in individuals with EvC syndrome [26]. Nevertheless, the spectrum of mutations characterized in the Chinese population still remains limited. In the present study, a novel variant (c.130delC, p.Leu44Phefs*72) and a previously reported EX9_11Del mutation in EVC1 were identified in an affected Chinese fetus. According to the ACMG standards, both the novel c.130delC variant and EX9_11Del were categorized as ‘Pathogenic’ (PVS1 + PM2 + PM3). The present study reports the 10th EVC1 mutation linked to EvC syndrome in the Chinese population. Notably, the present study was conducted on a single Chinese family, and the small sample size limits the generalizability of the findings regarding the prevalence and pathogenicity of this mutation in the broader Chinese population. In the present study, it was demonstrated that the EVC1 c.130delC variant may not impair transcriptional activity but could lead to the synthesis of a truncated protein in vitro, which is likely to constitute the underlying disease mechanism. However, it is important to note that there exits inherent limitations in overexpression experiments, as in vitro systems may not fully recapitulate the complexity of the in vivo environment. Given the rarity of the disorder

and the paucity of reported cases, further genetic confirmation in independent cohorts and functional assays are essential to definitively establish variant pathogenicity and elucidate the precise molecular mechanisms involved.

EvC syndrome contributes to a broad spectrum of phenotypic variability and involves multiple organ systems [27]. Postnatally, cardinal clinical features include short limbs and ribs, postaxial polydactyly, hypodontia, hypoplastic nails, fusion of the capitate and hamate bones, cone-shaped epiphyses of the phalanges, bowing of the humerus and proximal tibiofibular fusion [3]. The presence of congenital heart disease, a key determinant of life expectancy, can further support the diagnosis in some cases [28,29]. However, fetal phenotypes can be relatively nonspecific, and overt manifestations often do not become apparent until the third trimester, which poses a challenge for prenatal ultrasound evaluation and differential diagnosis in the early stages. To the best of our knowledge, prenatal abnormalities of EvC syndrome detectable after 18 gestational weeks primarily include narrow thorax, severe shortening of the long bones and hexadactyly of the hands and feet, which prompts consideration of short rib-polydactyly syndromes [30,31]. Nevertheless, definitive prenatal diagnosis of EvC syndrome by ultrasound evaluation is often hindered by limited information on comprehensive and characteristic fetal phenotypes. Consequently, while there is extensive literature on the postnatal diagnosis of EvC syndrome, dedicated clinical studies on its prenatal diagnosis remain limited. In the present case, routine fetal ultrasonography performed at 16+5 weeks gestation revealed only the cardinal manifestation of short limbs in EvC syndrome, which may be attributable to the relatively early gestational age and routine scanning methodology. More intensive ultrasound scanning during later gestational stages may reveal typical multi-system anomalies of EvC syndrome as fetal development progresses. In the present study, the definitive diagnosis of fetal EvC syndrome in the second trimester was established based on genetic analysis and subtle ultrasonographic findings. To the best of our knowledge, the present study represents the conclusive prenatal diagnosis of EvC syndrome established at the earliest gestational age and the third reported case of a prenatally diagnosed fetus in the Chinese population (12,16).

PGT has emerged as a pivotal technique in assisted reproductive technology, contributing to the achievement of successful pregnancies. Consequently, it has gained widespread adoption as a diagnostic tool in recent clinical practice [32,33]. PGT is categorized into three distinct subtypes, namely PGT for aneuploidies, for monogenic disorders and for structural rearrangements. It has now become a well-established alternative to conventional invasive prenatal diagnostic procedures [34,35]. The present study reported on a severe familial case involving three consecutive pregnancies complicated by fetal skeletal anomalies, which was confirmed as EvC syndrome by combined genetic diagnosis and subtle ultrasonographic findings at the second trimester. PGT was recommended to this family and brought the birth of a healthy male infant. This case highlights the clinical utility and feasibility of PGT, underscoring its potential for broader application in effectively preventing the recurrence of specific genetic disorders.

In summary, a novel pathogenic mutation in EVC1 was identified in a Chinese fetus. The findings of the present study broadened the established mutational spectrum of EvC syndrome and holds notable implications for the clinical management and genetic counseling of families affected by EvC.

Data Availability

The data generated and/or analyzed during this

study are available from the Figshare repository under the identifier [DOI10.6084/m9.figshare.29 17 8857 and DOI10.6084/m9.figshare.30353836].

Declarations

Ethics Approval and Consent to Participate

All procedures performed in this study were conducted in accordance with the ethical standards of the Declaration of Helsinki. The study protocol was approved by the Institutional Review Board of Jiangxi Maternal and Child Health Hospital (approval number: 20210324). Written informed consent was obtained from all participating patients.

Consent for Publication

Written informed consent for publication of their clinical details was obtained from all participants.

Availability of Data and Material

The data is not available to the public because of privacy. The corresponding author can be contacted if necessary.

Competing Interests

The authors declare that there is no conflict of interest.

Funding

This study was supported by National Natural Science Foundation of China (Grant No. 82160318 to YZ), Jiangxi Province Key Research and Development Project (Grant No. 20232BBG70023 to YZ), Youth Science Foundation of Jiangxi Province (Grant No. 20232BAB216025 to HL), Jiangxi Provincial Science and Technology Plan Projects of Traditional Chinese Medicine (Grant No. 20232B1258 to HL), Jiangxi Provincial Applied Research and Cultivation Program (Grant No. 20212BAG70007 to ZG) and Jiangxi Province Key Research and Development Project (Grant No. 20252BAC240535 to YY).

Authors' Contributions

Haiyan Luo contributed to the study design and manuscript writing. Zhen Guo performed the ultrasonography screening and Yao Yu conducted the prenatal diagnosis. Jia Chen and Qing Lu conducted the PGT analysis. Yan Yang, Ting Huang, Danping Liu assisted diagnosis of the disease and follow-up. Wangli Nie, Bicheng Yang, Jun Zou, Yanqiu Liu and Yongyi Zou provided guidance for the paper writing. All the authors have reviewed and approved the final manuscript.

Acknowledgements

We sincerely express our thanks to the family members for their participation in this study.

Authors' Imformation

The Department of Medical Genetics, Jiangxi Maternal and Child Health Hospital, Nanchang, 330006, Jiangxi Province, China

Haiyan Luo, Zhen Guo, Jia Chen, Qing Lu, Yan Yang, Ting Huang, Danping Liu, Yanqiu Liu, Bicheng Yang, Jun Zou, Yongyi Zou,

Jiujiang Polytechnic University of Science and Technology, Gongqing, 332020, Jiangxi Province , China

Yao Yu Jiujiang Maternal and Child Health Hospital, Jiujiang, 33200, Jiangxi Province, China

Wangli Nie,

References

1. Kalayci T, Altunoglu U, Çorbacioglu Esmer A, et al. Fetal skeletal dysplasia cohort of a single tertiary referral center in Istanbul, Turkey. Am J Med Genet A 2023;191:498-509.
2. MCKUSICK VA, EGELAND JA, ELDRIDGE R, et al. DWARFISM IN THE AMISH I. THE ELLIS-VAN CREVELD SYNDROME. Bull Johns Hopkins Hosp 1964 ;115:306-336.
3. Baujat G, Le Merrer M. Ellis-van Creveld syndrome. Orphanet J Rare Dis 2007;2:27.

4. Guschmann M, Horn D, Gasiorek-Wiens A, et al. Ellis-van Creveld syndrome: examination at 15 weeks' gestation. Prenat Diagn 1999;19: 879-883.
5. Zhuang J, Liu S, Wang J, et al. Prenatal whole exome sequencing identified two rare compound heterozygous variants in EVC2 causing Ellis-van Creveld syndrome. Mol Genet Genomic Med 2023:e2242.
6. Carss KJ, Hillman SC, Parthiban V, et al. Exome sequencing improves genetic diagnosis of structural fetal abnormalities revealed by ultrasound. Hum Mol Genet 2014 ;23:3269-3277.
7. Yang Y, Muzny DM, Xia F, et al. Molecular findings among patients referred for clinical whole-exome sequencing. JAMA 2014;312: 1870-1879.
8. Petrovski S, Aggarwal V, Giordano JL, et al. Whole-exome sequencing in the evaluation of fetal structural anomalies: a prospective cohort study. Lancet 2019;393:758-767.
9. Chandler N, Best S, Hayward J, et al. Rapid prenatal diagnosis using targeted exome sequencing: a cohort study to assess feasibility and potential impact on prenatal counseling and pregnancy management. Genet Med 2018 ;20:1430-1437.
10. Zhou X, Chandler N, Deng L, et al. Prenatal diagnosis of skeletal dysplasias using a targeted skeletal gene panel. Prenat Diagn 2018;38:692-699.
11. Peng Y, Yang S, Huang X, et al. Whole Exome Sequencing Analysis in Fetal Skeletal Dysplasia Detected by Ultrasonography: An Analysis of 38 Cases. Front Genet 2021;12: 728544.
12. Hao XY, Fan CN, He YH, et al. Prenatal Diagnosis of Ellis-van Creveld Syndrome by Targeted Sequencing. Chin Med J (Engl) 2016;129:1882-1883.
13. Shi L, Luo C, Ahmed MK, et al. Novel mutations in EVC cause aberrant splicing in Ellis-van Creveld syndrome. Mol Genet Genomics 2016;291:863-872.
14. Ren Y, You YQ, Zhou HH, et al. [Clinical analysis of 21 cases with short fetal femur in the third trimester]. Zhonghua Fu Chan Ke Za Zhi 2017;52:86-92.
15. Zhang W, Taylor SP, Ennis HA, et al. Expanding the genetic architecture and phenotypic spectrum in the skeletal ciliopathies. Hum Mutat 2018;39:152-166.
16. Huang X, Guo Y, Xu H, et al. Identification of a novel EVC variant in a Han-Chinese family with Ellis-van Creveld syndrome. Mol Genet Genomic Med 2019;7:e885.
17. Wang J, Wang X, Jia Y, et al. A homozygous EVC mutation in a prenatal fetus with Ellis-van Creveld syndrome. Mol Genet Genomic Med 2023;11:e2183.
18. Richards S, Aziz N, Bale S, et al. Standards and guidelines for the interpretation of sequence variants: a joint consensus recommendation of the American College of Medical Genetics and Genomics and the Association for Molecular Pathology. Genet Med 2015;17:405-424.
19. Umm-E-Kalsoom, Wasif N, Tariq M, et al. A novel missense mutation in the EVC gene underlies Ellis-van Creveld syndrome in a Pakistani family. Pediatr Int 2010;52:240-246.
20. Aziz A, Raza SI, Ali S, et al. Novel homozygous mutations in the EVC and EVC2 genes in two consanguineous families segregating autosomal recessive Ellis-van Creveld syndrome. Clin Dysmorphol 2016; 25 :1-6.
21. Blair HJ, Tompson S, Liu YN, et al. Evc2 is a positive modulator of Hedgehog signalling that interacts with Evc at the cilia membrane and is also found in the nucleus. BMC Biol 2011;9:14.
22. Pacheco M, Valencia M, Caparrós-Martín JA, et al. Evc works in chondrocytes and osteoblasts to regulate multiple aspects of growth plate development in the appendicular skeleton and cranial base. Bone 2012;50:28-

41.
23. Sund KL, Roelker S, Ramachandran V, et al. Analysis of Ellis van Creveld syndrome gene products: implications for cardiovascular development and disease. Hum Mol Genet 2009;18:1813-1824.
24. Ruiz-Perez VL, Blair HJ, Rodriguez-Andres ME, et al. Evc is a positive mediator of Ihh-regulated bone growth that localises at the base of chondrocyte cilia. Development 2007;134:2903-2912.
25. Ruiz-Perez VL, Ide SE, Strom TM, et al. Mutations in a new gene in Ellis-van Creveld syndrome and Weyers acrodental dysostosis. Nat Genet 2000;24:283-286.
26. Ruiz-Perez VL, Tompson SW, Blair HJ, et al. Mutations in two nonhomologous genes in a head-to-head configuration cause Ellis-van Creveld syndrome. Am J Hum Genet 2003;72 :728-732.
27. McKusick VA. Ellis-van Creveld syndrome and the Amish. Nat Genet 2000;24:203-204.
28. Blackburn MG, Belliveau RE. Ellis-van Creveld syndrome. A report of previously undescribed anomalies in two siblings. Am J Dis Child 1971;122:267-270.
29. Digilio MC, Marino B, Ammirati A, et al. Cardiac malformations in patients with oral-facial-skeletal syndromes: clinical similarities with heterotaxia. Am J Med Genet 1999;84:350-356.
30. Horigome H, Hamada H, Sohda S, et al. Prenatal ultrasonic diagnosis of a case of Ellis-van Creveld syndrome with a single atrium. Pediatr Radiol 1997;27:942-944.
31. Venkat-Raman N, Sebire NJ, Murphy KW, et al. Increased first-trimester fetal nuchal translucency thickness in association with chondroectodermal dysplasia (Ellis-Van Creveld syndrome). Ultrasound Obstet Gynecol 2005;25:412-414.
32. Harper JC, Aittomäki K, Borry P, et al. Recent developments in genetics and medically assisted reproduction: from research to clinical applications. Eur J Hum Genet 2018;26:12-33.
33. Fesahat F, Montazeri F, Hoseini SM. Preimplantation genetic testing in assisted reproduction technology. J Gynecol Obstet Hum Reprod 2020;49:101723.
34. Practice Committee of the Society for Assisted Reproductive Technology, Practice Committee of the American Society for Reproductive Medicine. Preimplantation genetic testing: a Practice Committee opinion. Fertil Steril 2007;88:1497-1504.
35. Greco E, Litwicka K, Minasi MG, et al. Preimplantation Genetic Testing: Where We Are Today. Int J Mol Sci 2020;21.